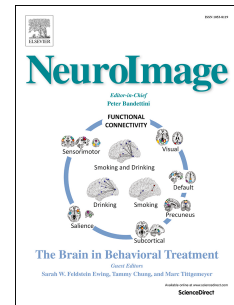# Accepted Manuscript

Resting-state functional connectivity predicts the ability to adapt to robot-mediated force fields

Irene Faiman, Sara Pizzamiglio, Duncan L. Turner

Please cite this article as: Faiman, I., Pizzamiglio, S., Turner, D.L., Resting-state functional connectivity predicts the ability to adapt to robot-mediated force fields, *NeuroImage* (2018), doi: 10.1016/j.neuroimage.2018.03.054.

Resting-state functional connectivity predicts the ability to adapt to robot-mediated force fields.

Irene Faiman[a, b], Sara Pizzamiglio[a] and Duncan L. Turner[a*]

[a] NeuroRehabilitation Unit, School of Health, Sport and Bioscience, College of Applied Health and Communities, University of East London, Water Lane, E15 4LZ London, United Kingdom.

[b] Faculty of Psychology and Neuroscience, Maastricht University, Universiteitssingel 40, 6229 ER Maastricht, Netherlands.

[*] Correspondence to Professor Duncan L. Turner at University of East London

E-mail address: d.l.turner@uel.ac.uk

ABSTRACT

Motor deficits are common outcomes of neurological conditions such as stroke. In order to design personalised motor rehabilitation programmes such as robot-assisted therapy, it would be advantageous to predict how a patient might respond to such treatment. Spontaneous neural activity has been observed to predict differences in the ability to learn a new motor behaviour in both healthy and stroke populations. This study investigated whether spontaneous resting-state functional connectivity could predict the degree of motor adaptation of right (dominant) upper limb reaching in response to a robot-mediated force field. Spontaneous neural activity was measured using resting-state electroencephalography (EEG) in healthy adults before a single session of motor adaptation. The degree of beta frequency (β; 15-25 Hz) resting-state functional connectivity between contralateral electrodes overlying the left primary motor cortex (M1) and the anterior prefrontal cortex (aPFC) could predict the subsequent degree of motor adaptation. This result provides novel evidence for the functional significance of resting-state synchronization dynamics in predicting the degree of motor adaptation in a healthy sample. This study constitutes a promising first step towards the identification of patients who will likely gain most from using robot-mediated upper limb rehabilitation training based on simple measures of spontaneous neural activity.

KEYWORDS

Electroencephalogram; resting-state; motor adaptation; robot-mediated force field; functional connectivity; partial least square regression.

HIGHLIGHTS

- Left M1-aPFC resting-state coherence predicts motor adaptation in a healthy sample
- Resting-state EEG coherence within the beta frequency band is the most predictive
- PLSR is feasible for studying correlation between neural activity and behaviour

1. INTRODUCTION

Motor learning can be divided into motor skill acquisition and motor adaptation. These phenomena can play different roles in the control of voluntary movements and are thought to be mediated by different neural substrates (Doyon et al., 2003). Motor adaptation results in a return to baseline levels of motor task performance following the occurrence of a movement error induced by an external perturbation or to changes in the body (Kitago & Krakauer, 2013). The study of motor adaptation often relies on systematic modification of the environment such as the imposition of external force fields or the rotation of the visual field within which a motor skill is executed (Doyon et al., 2009).

Robotic force field devices have gained popularity recently due to their relevance in rehabilitative interventions for patients with motor deficits (Patton & Mussa-Ivaldi, 2004; Scheidt & Stoeckmann, 2007). These can assist movements and document neurological and orthopaedic rehabilitation in early recovery stages (Reiner et al., 2005), whereas at more advanced stages they can introduce controlled force fields within the movement environment to increase task difficulty and potentially enhance neuroplasticity processes accompanying recovery (Turner et al., 2013). There have been changes in the design of individualised therapy with the development of prognostic models of motor recovery based on individual behavioural and imaging characteristics (Reinkensmeyer et al., 2016). Prognostic models may also be used to predict treatment effects (Cramer et al., 2007), thus providing an index of likelihood that a patient will respond to a specific rehabilitation training.

The capacity to learn a new motor ability also varies markedly across healthy individuals (Tubau et al., 2007) and differences in performance may be associated with the intrinsic dynamics of the brain (Linkenkaer-Hansen et al., 2001; Tomassini et al., 2011). Hence, many studies have examined spontaneous brain activity at rest in order to investigate how pre-existing differences at the neurophysiological level are reflected in differences in cognitive and behavioural performance (Kounios et al., 2008; Tambini et al., 2010; Matthewson et al., 2012). These findings have been extended to motor skill learning, where resting-state functional connectivity within the motor network and subtle interactions of this network with attentional networks could accurately predict performance gains (Wu et al., 2014; Mary et al., 2017). Furthermore, the inter-individual variability in motor adaptation to a force field task could be predicted from measures of resting-state beta frequency power in parieto-occipital and frontal regions collected before the adaptation session (Ozdenizci et al., 2017).

Measures of local activity are not the only relevant indices of neural functioning. Additional information on brain-behaviour dynamics could be obtained by investigating the efficiency of communication between functionally connected areas. It is acknowledged that brain function is not the result of several modular parts, but instead works as a complex network. Efficiency of communication within these networks predicts (motor) behaviour (Wu et al., 2014; Youssofzadeh et al., 2016; Della-Maggiore & McIntosh, 2005) and disruption of these networks is associated with deficits in motor performance (Wu et al., 2015; Carter et al., 2010). Therefore,

3

investigating the efficiency of resting-state synchronization patterns could provide novel insight into the individual neural differences underpinning successful motor adaptation.

In this study, we investigated whether spontaneous measures of neural activity could be predictive of an index of motor adaptation. Spontaneous neural activity was measured using resting-state electroencephalography (EEG) prior to motor adaptation of upper limb reaching in response to a robot-mediated force field. The motor adaptation paradigm employed in the current study has been extensively used in previous work (Pizzamiglio et al., 2017; Ozdenizci et al., 2017; Huang et al., 2012; Scheidt & Stoeckmann, 2007; Patton & Mussa-Ivaldi, 2004; Shadmehr & Holcomb, 1997). To the authors' best knowledge, examination of EEG resting-state coherence dynamics in this context is a novel approach that has not been previously implemented.

As oscillations in the beta frequency range (15-30 Hz) appear important for motor functions (Wu et al., 2014; Ozdenizci et al., 2017; Engel & Fries, 2010), we hypothesised that measures of beta frequency functional connectivity were predictive of motor adaptation performance. Furthermore, we aimed at replicating the finding that the magnitude of beta band power is predictive of the degree of motor adaptation (Ozdenizci et al., 2017). An exploratory approach was adopted to investigate whether measures of spontaneous activity within other frequency bands could also predict behavioural performance and whether differences in prediction could be demonstrated between eyes-closed and eyes-open resting-states.

2. MATERIAL AND METHODS

2.1 Participants

Sample size was determined a priori by referring to relevant previous studies (Wu et al., 2014; Ozdenizci et al., 2017). This was fix to a minimum of twenty, plus three to account for possible exclusions. Twenty-three healthy young adults with no history of neurological or musculoskeletal disorders volunteered in the study and gave their written informed consent (6 males and 17 females; age: mean ± standard deviation (SD) = 28 ± 7). All were right-handed and had normal or corrected-to-normal vision. The study was approved by the University of East London Ethical Committee (UREC_1415_29) and was conducted according to the Declaration of Helsinki (World Medical Association, 2002). Two participants were excluded due to inability to accomplish reaching movement timing, which led to excessive error trials. One was excluded due to a long interruption in the experiment. One was excluded because s/he reported suffering a psychiatric condition whilst undertaking the experiment. Hence, data from 19 participants (6 males, 13 females; age: 28 ± 8) were used.

2.2 Experimental Task and Design

Experiments were carried out in one continuous session. Participants sat in a comfortable chair in front of a shoulder/arm manipulandum workstation (MIT-Manus, Interactive Motion Technologies, Cambridge, MA, USA; Figure 1A). Shoulders were placed at the same height of the end-effector joystick and chair adjustments were

made to obtain a semi-pronated arm position with 70° shoulder extension and 120° elbow flexion. The forearm was supported by a custom-made thermoplastic trough for minimization of fatigue effects due to gravity. Safety belt straps were used to minimize trunk movements. Participants performed a reaching task with their dominant (right) arm by moving the joystick from a central starting point to a peripheral target, in a north-west-oriented reaching movement (135°). Visual online feedback of the joystick position was given through a vertical display screen situated at eye-level (Figure 1B). The starting point and the peripheral target consisted of black dots of 1 cm diameter measured on screen, with 15 cm actual linear distance. Instructions were to perform the movement within 1.0 to 1.2 seconds from the appearance of a visual cue (peripheral target turning red) and to stay on the target until robot-assisted arm relocation occurred. The latter was chosen for the returning movement so as not to interfere with the motor adaptation process. Feedback on reaching time was displayed after each trial.
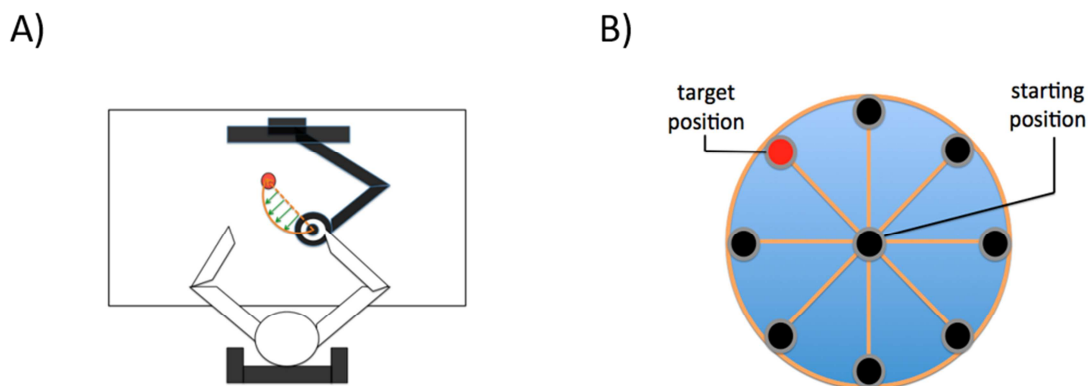
Figure 1. Task and experimental set-up. A) Schematic representation of the experimental setup. In order to perform the task, participants had to move the end-effector joystick towards the North-West 135° direction while visual feedback of their position was given on the screen. Green arrows represent the direction of the force field during the motor adaptation condition. The orange dashed line represents the ideal reaching trajectory, while the orange continuous line represents the trajectory deviation due to the force field in the early trials of motor adaptation. **.** B) Motor task requiring the participant to reach towards a peripheral target from a central starting position.

Participants performed the task in three experimental conditions, each including 96 reaching trials (Figure 2). The first and the third conditions, "Familiarization" and "Wash-Out" consisted of performing the reaching task in a null force field. In the second condition, "Motor Adaptation" (MA), the robot applied a counter-clockwise velocity-dependent force field of 25 Newton-second per meter (Ns/m), perpendicular to the 135° reaching trajectory. In between conditions, a period of rest was undertaken when 6 minutes of resting-state (RS) data were collected (3 minutes with eyes open – EO, and 3 minutes with eyes closed - EC, in a randomized order across participants but in constant order within subjects). The resting-state condition immediately preceding MA will be referred to as pre-MA (Pre-Motor Adaptation). Pre-MA eyes open and eyes closed RS-EEG data only have been analysed for the purpose of the present study. Other RS conditions have been introduced to investigate a separate hypothesis that is beyond the purpose of the present study, and results will be published elsewhere.
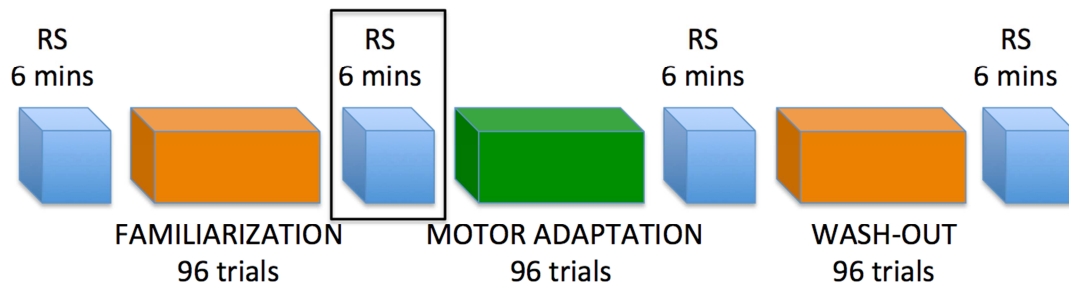
Figure 2. Experimental design. Coloured blocks represent the three experimental conditions. The orange colour indicates conditions of null force field, while the green colour indicates that a force field was applied in that condition. Six minutes resting-state EEG (blue blocks) was recorded in between experimental blocks. Only EEG data obtained during the pre-Motor Adaptation resting-state condition was used in this study (framed condition).

2.3 Data Acquisition

Neural activity and kinematic measures were simultaneously recorded during the whole experiment. Electroencephalographic activity was recorded (EEG; μV) using a high-density 64-channel Waveguard cap (ANT Neuro, Enschede, Netherlands). EEG electrodes were arranged according to the International 10-20 System (Jasper, 1958). Data were amplified with a TMSi Refa Ext amplifier (ANT Neuro, Enschede, Netherlands), digitized at 1024 Hz, and band-pass filtered from 0.1 to 500 Hz. Impedance was kept below 5 kΩ. During recordings, the Fz electrode was used as a reference. Kinematic measures were obtained from the automatic recordings of the robotic device and included end-effector position and velocity (along the x and y axes) and exerted forces (along x, y and z axes). Kinematic data were sampled at 200 Hz and stored for off-line analysis. The two signals were synchronized by a TTL pulse signal emitted by the robotic device in correspondence of each visual cue and transmitted to the EEG recording system via a BNC cable.

2.4 Measures of kinematic performance and neural activity

2.4.1 Kinematic measure of performance

Motor performance was quantified with a measure of trajectory error in each trial. Summed Error (SumErr; cm) was derived from raw kinematic data and is the sum of the observed deviations from the ideal linear trajectory (between the starting position and target position) for every time sample from movement onset (t_{on}, first time point at which velocity, $V > 0.03$m/s) to movement offset (t_{off}, first time point after movement onset at which velocity, $V < 0.03$m/s). Average SumErr scores were computed for trials 2-6 (T1) and for the last 5 trials (T2) for each participant during the MA condition (Trewartha et al., 2014). The percentage of improvement (PI) in motor adaptation performance was then computed for each participant as: PI = [(T2-T1)/T1]*100. This represents a quantitative measure of adaptation learning (i.e. amount of adaptation or behavioural gain). Measures derived by the SumErr index have been extensively used as dependent variables in previous studies (Pizzamiglio et al., 2017; Hunter et al., 2009; Burciu et al., 2014; Osu et al., 2003).

2.4.2 EEG measures of neural activity

Eyes-open and eyes-closed EEG data collected immediately before motor adaptation (Pre-MA) were used to predict performance. This is in line with previous studies that used resting-state immediately before task for behavioural prediction (Wu et al., 2014; Ozdenici et al., 2014; Cassady et al., 2017; Youssofzadeh et al., 2016; Mehrkanoon et al., 2016). The Familiarization condition was not analysed but served as a common prior state to minimize uncontrolled variability. Variability in participant brain states prior to resting-state data collection could give rise to inflated variance in the strength of connectivity measures, and introducing a standardized prior state common to all participants has been suggested to minimize variability due to uncontrolled variables (Tailby et al., 2015).

2.4.2.1 EEG data Pre-processing

Offline pre-processing was performed using the EEGLab analysis toolbox for MatLab 2015a (The MathWorks, Inc.;). As a laboratory standard procedure, data were filtered with a bandpass filter (0.5 – 100 Hz, FIR) and a notch filter (50 Hz, FIR). A secondary notch filter (25 Hz) was applied to correct for laboratory-related noise. Data were visually inspected to remove non-stereotyped artefacts and identify noisy channels. Bad channels were removed and data were re-referenced to the common average reference (Ludwig et al., 2009). Independent component analysis (ICA; Hyvärinen et al., 2004) implementing the extended Infomax algorithm (Lee et al., 1999) was run to remove stereotyped artefacts (e.g. eye blinks, muscles contractions), following criteria described in Chaumon et al. (2015). In the presence of residual artefacts after ICA, correspondence between EEG noise and activation of ambiguous components was investigated by plotting components in time. This method allowed accurate individuation of artefactual components that were ambiguous in a first analysis. Channels that were removed before ICA were replaced by spherical interpolation using neighbouring channels (6 channels per participant interpolated on average). Data were re-referenced to the common average. The EEG was segmented into 2 seconds epochs after preliminary investigation on what epoch length was the most robust for running a spectral analysis on our data.

2.4.2.2 Spectral Analysis of EEG data

For all channels, spectral information (i.e. frequency domain) within the data was extracted by means of a Fast Fourier Transformation (FFT) as implemented in FieldTrip toolbox for Matlab (Oostenveld et al., 2011). The FFT was run through a multi-taper method with a single (Hanning) taper window applied to reduce spectral leakage (Harris, 1978). Frequency resolution was set to 0.5 Hz (resulting in a time window of 2 sec) and a sliding window was set to 0.5 sec (Babiloni et al., 2010). The power density spectrum (μV^2) was obtained as an output of the FFT per each participant and condition (Storey, 2002). For subsequent analyses, band frequencies of interest were defined as follows: δ (2-4Hz), θ (4-8Hz), α (8-13Hz), β (13-30Hz), γ (30-60Hz), in keeping with previous studies (Babiloni et al., 2010).

Coherence is a measure of synchronization between each pair of channels and indicates the functional relationship between different brain regions (Bowyer, 2016). It is calculated as a squared correlation coefficient and gives a zero-to-one measure of the consistency of the phase difference between pairs of signals at a given frequency. The coherence spectrum was obtained from Fast Fourier transformed-data through the following formula:

$$C_{xy}(f) = \frac{|\Sigma_{i=1}^{L} S_{xy_i}(f)|^2}{\left(\Sigma_{i=1}^{L} S_{xx_i}\right) * \left(\Sigma_{i=1}^{L} S_{yy_i}\right)}$$

where C_{xy} represents coherence between two signals (x and y), f represents the specific frequency bin at which coherence is evaluated, S_{xy} represents the cross-spectra, S_{yy} and S_{xx} the auto-spectra, and L the number of trials evaluated. A seed region of interest was defined *a priori* based on the existing literature on motor adaptation (Hunter et al., 2009; Gandolla et al., 2014; Doyon et al., 2003; Doyon et al., 2009; Debas et al., 2010; Gandolfo et al., 2000). This encompassed channels C1 and C3, which according to the 10-20 system (Jasper, 1958), are located over the left primary motor cortex (M1). We adopted an exploratory approach and investigated coherence between left M1 and all other EEG channels to identify any areas that are substantially involved in predicting motor adaptation performance.

2.5 Statistical Analysis

Our aim was to test whether resting-state spontaneous neural activity recorded before the MA condition (Pre-MA) is predictive of motor adaptation during the MA condition. Although our expectations focused on the predictive power of beta coherence measures (Wu et al., 2014), we also conducted an exploratory analysis of all frequencies and all channels to account for the scarcity of literature evidence. Therefore for each frequency band (δ, θ, α, β, γ) and each RS condition (EO, EC), we obtained: 1) a dataset of the mean power in pre-MA at each of the 62 channels for each participant and 2) a dataset of the mean coherence in pre-MA between left M1 and all other channels for each participant. This resulted in the creation of 20 datasets. Each of these was used as an input variable (i.e. X-variable) in a regression model, with PI being used as the dependent variable (i.e. Y-variable). Hence, a total of 20 independent regression models were tested.

In order to quantify inter-individual variability in motor adaptation performance, descriptive measures of percentage improvement (PI) at the motor adaptation task were computed.

2.5.1 Ordinary Least Square Regression

For neural prediction of behaviour, we first considered implementing an Ordinary Least Square Regression. This turned out not to be a feasible method for two reasons. First, the predictor variables (EEG channels) displayed high collinearity. EEG captures activity of common neural sources at different scalp locations, thus some predictors were highly correlated. Multicollinearity causes biased estimation of the standard error of regression coefficients, limiting conclusions on population values

8

(Farahani et al., 2010). Second, the number of predictors (62 channels) exceeded the number of cases (19 participants), which would cause model over-fitting (Austin & Steyerberg, 2015).

2.5.2 Partial Least Square Regression

Partial Least Square Regression (PLSR) is a method of projection to latent structures that finds the relevant linear subspace underlying two matrices, X (predictor variables) and Y (response variables), and uses it to model X while simultaneously predicting Y (Krishnan et al., 2011; Ng, 2013; Wold et al., 2001). In recent years, the PLSR method has gained interest due to its feasibility for handling datasets in which 1) the number of X-variables exceeds the number of cases, 2) the X-variables are multicollinear and 3) there are missing data. PLSR has been successfully implemented in several studies investigating brain-behavioural dynamics (e.g. Wu et al., 2014; Wu et al., 2015; Mehrkanoon et al., 2016). PLSR determines orthogonal latent variables so that their covariance with Y is maximized (Krishnan et al, 2011). Component selection is an important step to determine the most reasonable model complexity (Wold et al., 2001). Compared to other regression methods, PLSR has the highest predictive ability with the lowest model complexity (Yeniay & Goktas, 2002). Therefore, PLSR was considered the most feasible method and was implemented for our analysis.

2.5.3 Description of the Implemented Approach

A PLSR model was fit to the EEG data and the behavioural data (PI) using the "pls" and the "ggplot2" packages for R open source software (R core team, 2013). A separate model was generated for each prepared dataset (see section 2.5) and specifically for each frequency band of interest and resting-state condition (EO/EC). For each model, PLSR was run twice. First, an Orthogonal Signal Corrected-PLSR (OSC-PLSR) was run on the whole set of channels (step 1). Then, a threshold selection method on regression coefficients was used to individuate the subset of channels that made the most substantial contribution to the model (variable reduction; step 2). Lastly, a second PLSR model was fitted to the significantly informative variables (step 3) and performance was measured (step 4). Ordinary Least Square Regression was run as a control analysis (step 5). Figure 3 describes the flow of the self-implemented method; steps are described in detail in the next paragraphs.
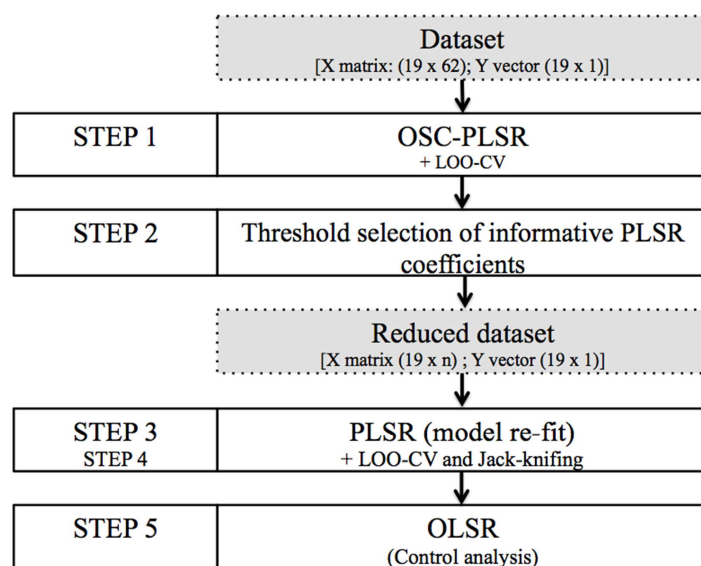
Figure 3. Statistical analysis steps. STEP 1 and STEP 2. Orthogonal signal-corrected Partial Least Square Regression (OSC-PLSR) and threshold selection were implemented as variable reduction method to create a reduced dataset just containing informative variables. STEP 3 and STEP 4. Once a reduced dataset was obtained (n = number of channels that passed the threshold selection), a second PLSR model was fitted to the data and performance was measured by means of leave-one-out cross validation (LOOCV) and jack-knifing. STEP 5. As a control analysis, an Ordinary Least Square Regression (OLSR) was run.

Step 1. OSC-PLSR.

Step 1.1 Data preparation.

Before the analysis, precautions were taken to obtain unbiased estimates of the regression coefficients, which have been then used as a reference for selecting influential variables in the PLSR model (see Step 2). These included data scaling and centring and application of an Orthogonal Signal Correction procedure to the X-variables (Wold et al., 2001; Wold et al., 1998). All pre-processing steps were conducted agnostically to the test set.

Data scaling and centring. Input variables were scaled to unit variance and mean centred. By linear rescaling, variables are weighted to be attributed the same prior importance in the PLS analysis (Wold et al., 2001). This allows a direct comparison of regression coefficients of the model, facilitating the individuation of the most predictive variables (Gelman, 2008). This is useful when it is not possible to make *a priori* assumptions on the relative importance of each X-variable for the model, as in our exploratory analysis on regression coefficients.

Orthogonal signal correction. Orthogonal signal correction was applied to the predictor matrix X in order to minimize bias of the PLSR coefficients. Orthogonal variation has been shown to have a strong impact on the regression coefficients by biasing their estimated values and thus the interpretation of predictors' importance in the model (Trygg & Wold, 2002). Orthogonal signal correction consists of removing from the X-matrix a small number of factors that account for as much as possible of the variation in X and are orthogonal to Y, eliminating bias (Wold et al., 1998).

10

Step 1.2 PLSR Analysis.

Model details. OSC-PLSR was run by implementing an OSC adapted formula (Wehrens, 2011) and the orthogonal scores algorithm (Martens & Næs, 1989). The whole set of channels was used as X-variables and PI scores were used as the Y-variable. Models with different number of components (1 to 17) were compared and the reasonable number of components to retain in the model was determined. Relevant indices (regression coefficients, indices of fit) were saved for further analysis.

Determining the most reasonable number of components. A model was selected that included as many components as needed to explain at least the 80% of variance in Y (Wu et al., 2014, Krishnan et al., 2013). Along with this, the root mean square error of prediction (RMSEP), the cross-validated R squared (Q Squared) and model parsimony were taken into account. In trade-off cases, in which choosing a less parsimonious model would have led to a better fit (higher Q Squared, lower error), this was investigated in parallel with the more parsimonious one, and resulting PLSR coefficients were compared. The process of component selection was agnostic to the test set.

Step 2. Variable reduction method.

When investigating the predictive power of large numbers of variables in complex systems, data reduction through projection methods and/or variable selection methods is necessary for improving prediction and interpretation (Mehmood et al., 2012). In our analysis, the first PLSR model (OSC-PLSR) was fit to this end (Maitra & Yan, 2008). Different approaches exist (see Mehmood et al., 2012 for a review). The variable reduction method implemented in this study is inspired by PLS wrapper methods (Mehmood et al., 2012), in particular to the backward variable selection PLS (BVSPLS; Pierna et al., 2009) and to the threshold method on regression coefficients implemented by Wu et al. (2014).
The most informative X-variables were found based on a threshold selection method on z-transformed PLSR coefficients. PLSR coefficients constitute a measure of association between each X-variable and the Y-variable. Standardized coefficients identify the importance of each X-variable in the model. Coefficients that exceeded the 95% confidence interval of the PLS coefficients vector were identified, then plotted on the EEG channels layout and visually inspected. Since we expected about 3 out of 62 coefficients to pass the significance threshold by chance (5% false positive rate), significantly informative X-variables were selected for further modelling just if they clustered to constitute an area of two or more spatially contiguous channels.

Step 3. PLSR model re-fitting.

After selection, the least informative X-variables were excluded from the model, and a second PLSR model just including the significant and contiguous channels was fitted. If needed, further elimination of the least informative variables was performed by means of backward stepwise method (Draper & Smith, 2014; removal criterion: jack-knife p>.05) until the best PLSR model was obtained where all X-variables made

significant contribution to the Y-variable prediction. Relevant indices of the re-fitted model were extracted for interpretation purposes.

Step 4. Model evaluation.

Cross-validation. Leave-one-out cross-validation (LOOCV) was used to estimate the model's prediction error (Wakeling & Morris, 1993; Clark & Cramer, 1993). LOOCV is a computer-based re-sampling technique consisting in the iterative removal of one participant from the whole sample, and subsequent fit of a PLSR model to the n-1 sample. The Y-variable of the excluded participant is then predicted by the model based on the participant's X-variables. Deviation between the predicted and the actual Y-variable of the left-out participant is measured for each of the n-1 samples. The predictive ability of the model is summarized in the cross-validated R^2 index, named Q^2 and defined as:

$$Q^2 = \frac{SD - PRESS}{SD}$$

with SD representing the "squared deviations of each dependent value from the mean of all dependent values" and PRESS representing the predictive residual sum of squares, which is "the sum of the squared deviations between the actual and predicted dependent values computed during the cross validation runs" (Clark & Cramer, 1993). Unlike the R^2 index, which is specific to the data sample, Q^2 gives a measure of how much Y-variance can be explained from the leave-one-out predictions, thus providing a formal test of the PLSR model's predictive ability. A $Q^2 < 0$ indicates a poor model. A $Q^2 = 0$ indicates that the model is not better than a mean model. A $Q^2 > 0$ indicates that the model's predictive ability is better than a mean model, since the average prediction error is lower than the squared deviation of the original dependent values. There is no clear cut-off value for establishing whether a PLSR model is significantly better than a mean model in predicting Y. Some consider a model including n component satisfactory already when $Q^2 > 0$ (Documentation, Statistica). Others concluded that any Q^2 value greater than 0.25 can be accepted as very unlikely to have resulted from chance correlation - when n>12 (Clark & Cramer, 1993). Hence, models with $Q^2 > 0$ have been considered satisfactory. Models with $Q^2 > 0.25$ have been considered very strong prediction models. The Jack-knifing test was used as a second indicator of model significance.

Jack-knifing. Jack-knife test was run to test significance of X-variables' contribution to the model's prediction. Through Jack-knifing, standard errors are derived from the variation in the parameters of the many sub-models obtained during cross-validation. Their t-distribution is then used to derive confidence intervals (Wold, 1982; Martens & Martens, 2000). Although jack-knifing is outperformed by bootstrapping methods in many statistical settings, this technique is thought to perform well in PLSR, since all PLSR parameters are close to normally distributed (Wold et al., 2001).

Pearson product-moment correlation. For each model, the Pearson product-moment correlation coefficient was computed to provide a measure of relationship strength between Y observed and predicted values (Rodgers & Nicewanders, 1988).

Permutation-based p-values for the Pearson product-moment correlation coefficients were derived (999 permutations conducted).

Step 5. Control analysis.

As a control analysis, Ordinary Least Square Regression was run on the reduced dataset.

3. RESULTS

3.1 Kinematic measures of performance

Descriptive measures of kinematic performance indicated high inter-individual variability in Percentage Improvement during the motor adaptation task (*M*= -59.79, *SD* = 18,35; Table 1). A probability density graph visually displaying the frequency distribution of PI is reported in Figure 4.

N	Mean	*SD*	Range	
			Min.	Max.
19	-59,79	18,35	-83,02	-18,88

Table 1. Descriptive statistics. Sample descriptive statistics for kinematic measures of Percentage Improvement (PI). *N* = number of participants; *SD* = Standard Deviation; Min. = Minimum; Max. = Maximum.
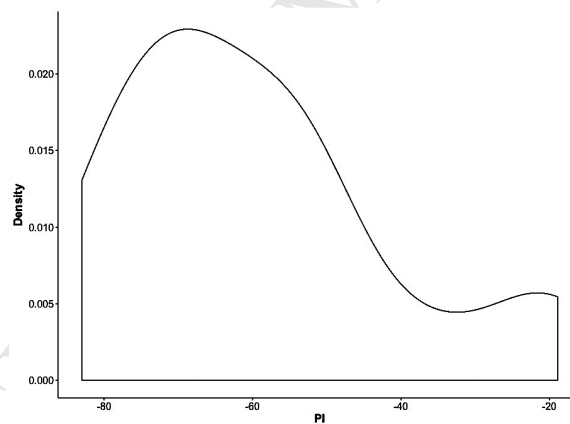
Figure 4. Probability density graph. The graph displays the sample probability density (y axis) for kinematic measures of Percentage Improvement (PI; x axis).

3.2 PLSR Analysis

Resting-state measures of EEG power and M1 coherence recorded immediately before task (Pre-MA condition) were entered in independent PLSR models to predict Percentage Improvement (PI) during motor adaptation. Within our variable reduction method, an average of 2.75 PLSR coefficients per model passed the 95% CI threshold. Of these, coefficients clustered together in 10 of the 20 models tested. These 10 models were further analysed by fitting a PLSR model to the reduced set of X-variables, i.e. EEG channels (Table1). In those cases in which regression coefficients of the same EEG channels were compared across models with different

number of components (see section 2.5.2, Step 1.2), no differences were detected in the coefficients exceeding the 95% CI. Since the same influential EEG channels were identified, these were selected as input variables of the second PLSR models.

By refitting a PLSR model to the set of EEG channels individuated through our variable reduction method, significant predictors of motor adaptation performance were identified. Significant predictors of performance were coherence between channels overlying left M1 and channels overlying the left prefrontal cortex (FP1, FPZ) within the β-band for the eyes-open condition, and within the β- and γ-bands for the eyes-closed condition.

Model prediction accuracy was evaluated by means of LOOCV and by means of a Jack-knife test of significance that was carried out on the EEG channels. 85% of the variance in M1-left prefrontal β coherence (eyes-closed condition) explained 25% of the variance in PI ($Q^2 = 0.25$, RMSEP = 15.51, $R^2 = 0.37$. Jack-knife on FP1: $t(18) = -4.88$, p < .001; Jack-knife on FPZ: $t(18) = -3.58$, p < .01), whereas 84% of the variance in γ-coherence (eyes-closed condition) explained 11% of the variance in PI ($Q^2 = 0.11$, RMSEP = 16.81, $R^2 = 0.29$. Jack-knife on FP1: $t(18) = -2.77$, p <.05; Jack-knife on FPZ: $t(18) = -2.38$, p < .05). M1-FPZ β coherence (eyes-open condition) explained 13% of the variance in PI ($Q^2 = 0.13$, RMSEP = 16.69, $R^2 = 0.27$).

Separate PLSR models assessing the prediction power of left M1 coherence in other frequency bands generated models that predicted performance not better than an intercept model. The same was true for measures of resting-state power. Results for the 10 models individuated through our variable reduction method are reported in Table 2.

Pearson product-moment correlation between observed and predicted values of PI indicated significant positive correlation for the eyes-closed M1-left prefrontal β coherence condition, $r = 0.51$ (p < .05). Correlations between observed and predicted values for the other models yielded no statistically significant results.

Condition	Model	N Comp	X var.	RMSEP	Q^2	r	Channels
Pow θ EC		2	99,81	20,90	-0,3686	.187	P5, PO3, PO5
Pow α EC		1	95,65	20,05	-0,2592	-.057	O2, PO6, PO8
Pow β EC		1	93,02	19,61	-0,2049	-.178	P7, PO5
Pow θ EO		1	78,00	19,93	-0,2448	-.159	T8, TP8
Pow α EO		2	99,00	20,80	-0,3552	-.151	P7, PO7, O2, PO8
Coh α EC		1	98,53	19,15	-0,1488	-.114	PO6, PO8
Coh β EC	1	1	58,15	16,06	0,1918	.465	AF3, FP1***, FPZ**
	2	**1**	**84,94**	**15,51**	**0,2462**	**.515***	**FP1***, FPZ****
Coh γ EC	1	1	53,57	16,99	0,0956	.366	FP2, AF3, FP1*, FPZ*
	2	1	74,38	17,10	0,0839	.356	FP2, FP1*, FPZ*
	3	**1**	**83,78**	**16,81**	**0,1146**	**.388**	**FP1*, FPZ***
Coh β EO	1	2	100,0	16,98	0,0963	.309	AF3, FPZ**
	2	**1**	**100,0**	**16,69**	**0,1268**	**.383**	**FPZ**
Coh γ EO		1	65,75	21,25	-0,4152	-.174	CP2, CP4, C6, C4

Table 2. Prediction of motor adaptation performance. Condition: Pow = power recorded at channels reported in the last column; Coh = left M1 coherence with the channels reported in the last column; EC = eyes-closed condition; EO = eyes-open condition. Model = for each condition, models that were further reduced by means of backwards elimination of non-significant channels are reported, and presented over multiple rows. N Comp = number of components retained in the PLSR model. X var. = percentage of X-variance explained by the model. RMSEP = Root Mean Square Error of Prediction. Q^2 = Cross-Validated R^2. r = Pearson product-moment correlation coefficient for observed and predicted values. Within this column: * = permutation-based significance value for the Pearson correlation coefficient p<.05. Channels = EEG channels individuated through our variable reduction method that have been entered as X-variables in the PLSR model. Within this column: * = Jack-knife test p<.05; ** = Jack-knife test p<.01; *** = Jack-knife test p<.001. The best predictive models of motor adaptation are highlighted in bold characters.

3.3 Control Analysis (Ordinary Least Square Regression)

When the EEG channels identified by the PLSR were used as predictors in an Ordinary Least Square Regression, results showed that β-coherence measures of both the eyes-closed and eyes-open conditions significantly predicted performance (eyes-closed r = 0.61; R^2 = 0.38; F(2,16) = 4.86; p <.05; eyes-open r = 0.52; R^2 = 0.27; F(1,17) = 6.16; p <.05). These results are in line with prediction models detected through the PLSR method. On the other hand, γ- coherence generated a model that had no significant prediction value (r = 0.55; R^2 = 0.31; F(2,16) = 3.53; p >.05) . This result contradicts the PLSR results. This may be due to the presence of a very small effect in γ, which has been detected by a PLSR model of one component, but was lacking in prediction power when the two predictors (FP1, FPZ) were entered separately in an OLSR model. Table 3 summarizes the three OLSR models. Scatterplots are reported in Figure 5.

		B	SE B	Standardized B
β-coherence EC	Constant	- 30.65	10.12	
	FP1	- 29.23	46.10	- .17*
	FPZ	- 77.23	44.51	- .47*
β-coherence EO	Constant	- 36.85	9.95	
	FPZ	- 83.90	33.80	- .52*
γ-coherence EC	Constant	- 38.39	9.04	
	FP1	- 92.22	52.68	- .50
	FPZ	- 11.82	43.41	- .08

Table 3. Ordinary Least Square Regression models. For each of the three models independently tested, unstandardized coefficients values (B), standard errors (SE B) and standardized coefficients values (Standardized B) are displayed. Note that higher *negative* PI values represent higher degree of motor adaptation (see section 2.4.1 for details on PI computation). Hence, negative B values point to a positive linear relation with PI. * = predictor with significance value p <.05.

β-coherence EC

β-coherence EO

γ-coherence EC
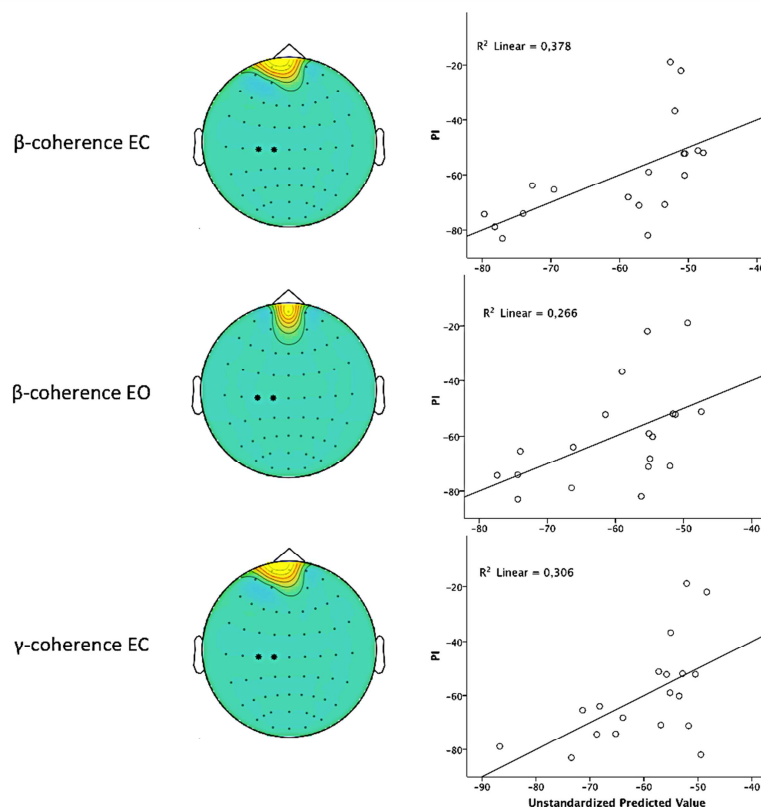
Figure 5. Ordinary Least Square Regression scatterplots. For each of the significant models, reported are a scatterplot of the regression of neural resting-state measures on behavioural performance (PI= Percentage of Improvement), and the associated topographic representation of significant regression coefficients derived from the PLS model. Asterisks = channels taken as seed region for M1.

4. DISCUSSION

4.1 Overview and novel findings

The present study investigated whether individual differences in the intrinsic dynamics of the brain can predict the magnitude of motor adaptation in healthy subjects. We demonstrated that individual measures of resting-state functional coupling between left M1 and the anterior prefrontal cortex (aPFC) predicted the degree of motor adaptation. Resting-state power measures had no predictive value for motor adaptation.

These results are in line with previous studies that, using different paradigms and neuroimaging methods such as fMRI (Landi et al., 2011; Vahdat et al., 2011), EEG (Molteni et al., 2012; Youssofzadeh et al., 2016; Ozdenizci et al., 2017) and PET (Krebs et al., 1998; Krakauer et al., 2004; Della-Maggiore & McIntosh, 2005), consistently demonstrated cortical activation of the prefrontal cortex (PFC) and M1 during motor adaptation tasks. Our study extends these findings by showing that efficiency of resting-state communication between specific areas of this network is an essential prerequisite for successful motor adaptation. These findings are more extensively discussed in the following sections.

16

4.2 Resting-state cortical connectivity predicts motor adaptation performance.

Recent studies have demonstrated that resting-state functional connectivity dynamics can explain a considerable amount of variation in behavioural performance, such as motor skill learning (Wu et al., 2014) and cognitive performance (Kounios et al. 2008; Tambini et al., 2010). Our results add to these findings and intriguingly show that synchronization of neural oscillations of the brain at rest has clear functional significance as it predicts behaviour. In particular, we provide novel evidence for the key role of coherence between left M1 and the anterior prefrontal cortex (aPFC) in the prediction of motor adaptation. This finding is consistent with results of a recent study that, using partial Granger causality (PCG), found an increase in causal effects in the aPFC during motor adaptation in gait training (Youssofzadeh et al., 2016). Additionally, and in keeping with existing literature on motor behaviour, our exploratory analysis of different frequency bands revealed that activity within the β-range is the best neurophysiological correlate of motor behaviour. In fact, in the present study M1-aPFC connectivity within the β-band predicted 25% of the variance in motor adaptation in the eyes-closed condition, and 13% of behavioural variance in the eyes-open condition. Consistency of findings across conditions suggests that this is a highly reliable predictor of performance. The lower prediction strength observed in the eyes-open condition is likely to result as a consequence of the overall decrease in frontal coherence measured during eyes-open compared to eyes-closed resting-state (Boytsova & Danko, 2010). Eyes-closed M1-aPFC connectivity within the γ-frequency band was also found to be a significant predictor of motor adaptation, but with reduced prediction strength ($Q^2 = 0.11$). We believe that this effect is very small as its significance has not been confirmed by our control analysis using Ordinary Least Square Regression. In contrast, frequencies within the δ-, θ- and α-bands had no predictive value.

The aPFC has been associated with functions such as the explicit processing of internal states (Christoff & Gabrieli, 2000), the maintenance of a cognitive state necessary for memory retrieval (Tulving, 1985), prospective memory (i.e. the intention to carry out an action after a delay; Burgess et al., 2001), branching and reallocation of attention (Koechlin, 1999) and relational integration (i.e. the simultaneous consideration of multiple relations between objects or thoughts; Christoff et al., 2001). In an attempt to synthesize the multiple models of the aPFC, Ramnani and Owen (2004) proposed a specific role of this region for simultaneously considering multiple operations to be executed in the pursuit of a higher behavioural goal. This interpretation accounts well for, and encases all the functional features mentioned above. Within this theoretical framework, we believe that the M1-aPFC functional coupling underpinning successful motor adaptation is likely to represent a potential state of preparedness for the integration of multiple dimensions into a descending predictive model resulting in successful adaptive movements. According to the active inference theory, adapting to an external perturbation is thought to result from a tuning process during which the motor cortex (M1) generates top-down predictions of the proprioceptive consequences of movement, and subsequently updates these based on error feedback (Friston, 2009; Gandolla et al., 2014; Clark, 2015) In our motor adaptation task, the same behavioural outcome learned during the familiarization phase (linear reaching movement) has to be achieved in a new environmental context, and information on the learned movement, the current

17

movement, the desired movement, and the external force perturbation have to be brought together to create an exact descending prediction that fulfils the behavioural goal. Flexible communication between the M1 and the aPFC could facilitate adaptive behaviour by predisposing the creation of accurate prediction models that promptly integrate novel contextual information to the previously learned motor command.

4.3 Resting-state local power does not predict motor adaptation performance.

Based on the study of Ozdenizci et al. (2017), we aimed at replicating the finding that resting-state β-power in parieto-occipital and frontal regions is predictive of motor adaptation. However, resting-state power measures had no predictive value on the amount of adaptation in the present study. Discrepancy between findings may be due to methodological differences in the investigation of prediction. Ozdenizci and colleagues (2017) individuated principal components of resting-state activity at the group level, derived then the components' power spectrum for each participant, and eventually used these as predictors of motor adaptation performance in a regression model. On the other hand, we performed an independent component analysis for each participant and then tested the predictive power of noise-free activity recorded at the electrode-level. Power computed at the electrode level may not be a powerful enough measure for predicting behavioural outcomes, possibly due to its lower spatial resolution. In support of this claim, a previous study using a similar methodological approach to the one implemented in this work showed that cortical connectivity measures but not power measures were predictive of motor skill learning (Wu et al., 2014). Consequently, investigations of power measures using source-level techniques (as in the case of Ozdenizci et al., 2017) may prove to be more effective in predicting performance.

5. LIMITATIONS AND FUTURE DIRECTIONS

One limitation of this study is that EEG data were analysed at the electrode level, which limits the exact spatial localization of neural sources. The correspondence between location of electrodes on the scalp and the underlying brain structure could therefore be imperfect. However, the investigation of resting-state correlates of motor adaptation (and skill learning) is in its infancy and the present study constitutes a first, exploratory analysis of the topic using EEG. This complements other work that used electrode-level prediction models of behaviour (e.g. Wu et al., 2014). Future studies could use methods of projection to the source level to improve spatial resolution (Hassan et al., 2014).

About 70% of our population sample consisted of females. Literature suggests sex-specific dynamics in resting-state functional organization (Conrin et al., 2018; Salehi et al., 2017; Tian et al., 2011). Hence, we recognize the potential for a degree of gender bias in our results and these should be interpreted accordingly.

In keeping with previous work (Wu et al., 2014; Mehrkanoon et al., 2016), the present study demonstrated that PLSR provides a robust data-driven approach to identify the models that best predict behaviour. Results can be used to test *a priori* hypothesis in replication studies that, making use of independent datasets, would further substantiate the present results. Based on previous studies (Hunter et al., 2009; Gandolla et al., 2014; Doyon et al., 2009; Gandolfo et al., 2000), our hypothesis was

that M1 connectivity could be predictive of subsequent motor adaptation. However, we do not exclude that connectivity between other areas involved in the motor adaptation network could be predictive of performance. This possibility should be investigated in future, and methods designed for the analysis of complex network dynamics such as graph theory could be implemented. Future studies using different neuroimaging methods should also investigate the relationship between activity of cortical and subcortical structures, since the latter have been shown to have a significant role in motor adaptation (Della-Maggiore & McIntosh, 2005; Doyon et al., 2009). Regarding long-term clinical applications of our findings in a healthy sample, they could represent a first step towards the development of prognostic models to be used for assisting clinicians in their treatment choices (Cramer et al., 2007; Stinear, 2010; Reinkensmeyer et al., 2016). In this context, information on what the chances are of a patient responding to a particular rehabilitation training could be obtained based on simple measures of neural activity, collected time- and cost-effectively.

6. CONCLUSIONS

The present study provides novel evidence for the significance of resting-state functional connectivity in predicting the subsequent degree of motor adaptation in a healthy sample. Analysis of communication patterns in the resting brain revealed that communication between the primary motor cortex and the anterior prefrontal cortex via beta frequency coherence plays a substantial role in determining the degree of individual motor adaptation.
Predicting individual differences in motor adaptation has important implications for neurorehabilitation. Our delineation of prediction suggest the possibility of using simple measures of resting-state activity to identify patients who will likely benefit more from using robot-mediated upper limb rehabilitation training.

7. FUNDING

8. CONFLICTS OF INTEREST

Conflicts of interest: none.

9. AKNOWLEDGEMENTS

10. REFERENCES

Austin, P. C., & Steyerberg, E. W. (2015). The number of subjects per variable required in linear regression analyses. *Journal of clinical epidemiology*, *68*(6), 627-636. doi:10.1016/j.jclinepi.2014.12.014.

Babiloni, C., Marzano, N., Iacoboni, M., Infarinato, F., Aschieri, P., Buffo, P., ... & Del Percio, C. (2010). Resting state cortical rhythms in athletes: a high-resolution EEG study. *Brain research bulletin*, *81*(1), 149-156. doi:10.1016/j.brainresbull.2009.10.014.

Bowyer, S. M. (2016). Coherence a measure of the brain networks: past and present. *Neuropsychiatric Electrophysiology*, *2*(1), 1. doi:10.1186/s40810-015-0015-7.

Boytsova, Y. A., & Danko, S. G. (2010). EEG differences between resting states with eyes open and closed in darkness. *Human physiology*, *36*(3), 367-369. doi:10.1134/S0362119710030199.

Burciu, R. G., Reinold, J., Rabe, K., Wondzinski, E., Siebler, M., Müller, O., ... & Timmann, D. (2014). Structural correlates of motor adaptation deficits in patients with acute focal lesions of the cerebellum. *Experimental brain research*, *232*(9), 2847-2857. doi:10.1007/s00221-014-3956-3.

Burgess, P. W., Quayle, A., & Frith, C. D. (2001). Brain regions involved in prospective memory as determined by positron emission tomography. *Neuropsychologia*, *39*(6), 545-555. doi:10.1016/S0028-3932(00)00149-4.

Carter, A. R., Astafiev, S. V., Lang, C. E., Connor, L. T., Rengachary, J., Strube, M. J., ... & Corbetta, M. (2010). Resting interhemispheric functional magnetic resonance imaging connectivity predicts performance after stroke. *Annals of neurology*, *67*(3), 365-375. doi: 10.1002/ana.21905.

Cassady, K., Ruitenberg, M., Koppelmans, V., Reuter-Lorenz, P., De Dios, Y., Gadd, N., ... & Mulavara, A. (2017). Neural predictors of sensorimotor adaptation rate and savings. *Human brain mapping*. doi: 10.1002/hbm.23924

Chaumon, M., Bishop, D. V., & Busch, N. A. (2015). A practical guide to the selection of independent components of the electroencephalogram for artifact correction. *Journal of neuroscience methods*, *250*, 47-63. doi: 10.1016/j.jneumeth.2015.02.025.

Christoff, K., & Gabrieli, J. D. (2000). The frontopolar cortex and human cognition: evidence for a rostrocaudal hierarchical organization within the human prefrontal cortex.*Psychobiology*, *28*(2), 168-186. doi:10.3758/BF03331976.

Christoff, K., Prabhakaran, V., Dorfman, J., Zhao, Z., Kroger, J. K., Holyoak, K. J., & Gabrieli, J. D. (2001). Rostrolateral prefrontal cortex involvement in relational integration during reasoning. *Neuroimage*, *14*(5), 1136-1149. doi:10.1016/j.cortex.2010.04.008.

Clark, A. (2015). Surfing uncertainty: Prediction, action, and the embodied mind. *Oxford University Press.*

Clark, M., & Cramer, R. D. (1993). The probability of chance correlation using partial least squares (PLS). *Molecular Informatics*, *12*(2), 137-145. doi:10.1002/qsar.19930120205.

Conrin, S. D., Zhan, L., Morrissey, Z. D., Xing, M., Forbes, A., Maki, P., ... & Leow, A. D. (2018). Sex-by-age differences in the resting-state brain connectivity. *arXiv preprint arXiv:1801.01577*.

Cramer, S. C., Parrish, T. B., Levy, R. M., Stebbins, G. T., Ruland, S. D., Lowry, D. W., ... & Wilkinson, S. B. (2007). Predicting functional gains in a stroke trial. *Stroke*, *38*(7), 2108-2114. doi: 10.1161/STROKEAHA.107.485631.

Debas, K., Carrier, J., Orban, P., Barakat, M., Lungu, O., Vandewalle, G., ... & Benali, H. (2010). Brain plasticity related to the consolidation of motor sequence learning and motor adaptation. *Proceedings of the National Academy of Sciences*, *107*(41), 17839-17844. doi: 10.1073/pnas.1013176107.

Della-Maggiore, V., & McIntosh, A. R. (2005). Time course of changes in brain activity and functional connectivity associated with long-term adaptation to a rotational transformation. *Journal of neurophysiology*, *93*(4), 2254-2262. doi:10.1152/jn.00984.2004.

Documentation, Statistica. "Principal Component Analysis (PCA) and Partial Least Squares (PLS) Technical Notes." *Documentation.statsoft.com*. N.p., n.d. Web. 12 May 2017.<http://documentation.statsoft.com/STATISTICAHelp.aspx?path=mspc%2FPCAandPLSTechnicalDetails>.

Doyon, J., Bellec, P., Amsel, R., Penhune, V., Monchi, O., Carrier, J., ... & Benali, H. (2009). Contributions of the basal ganglia and functionally related brain structures to motor learning. *Behavioural brain research*, *199*(1), 61-75. doi: 10.1016/j.bbr.2008.11.012.

Doyon, J., Penhune, V., & Ungerleider, L. G. (2003). Distinct contribution of the cortico-striatal and cortico-cerebellar systems to motor skill learning. *Neuropsychologia*, *41*(3), 252-262. doi:10.1016/S0028-3932(02)00158-6.

Draper, N. R., & Smith, H. (2014). *Applied regression analysis*(Vol. 326). John Wiley & Sons.

Engel, A. K., & Fries, P. (2010). Beta-band oscillations—signalling the status quo?. *Current opinion in neurobiology*, *20*(2), 156-165. doi: 10.1016/j.conb.2010.02.015.

Farahani, H. A., Rahiminezhad, A., & Same, L. (2010). A Comparison of Partial Least Squares (PLS) and Ordinary Least Squares (OLS) regressions in predicting of couples mental health based on their communicational patterns. Procedia-Social and Behavioral Sciences, 5, 1459-1463. doi:10.1016/j.sbspro.2010.07.308.

Friston, K. J., Daunizeau, J., & Kiebel, S. J. (2009). Reinforcement learning or active inference?. PloS one, 4(7), e6421. doi: 10.1371/journal.pone.0006421.

Gandolfo, F., Li, C. S., Benda, B. J., Schioppa, C. P., & Bizzi, E. (2000). Cortical correlates of learning in monkeys adapting to a new dynamical environment. *Proceedings of the National Academy of Sciences*, *97*(5), 2259-2263. doi: 10.1073/pnas.040567097.

Gandolla, M., Ferrante, S., Molteni, F., Guanziroli, E., Frattini, T., Martegani, A., ... & Ward, N. S. (2014). Re-thinking the role of motor cortex: context-sensitive motor outputs?. *NeuroImage*, *91*, 366-374. doi: 10.1016/j.neuroimage.2014.01.011.

Gelman, A. (2008). Scaling regression inputs by dividing by two standard deviations. *Statistics in medicine*, *27*(15), 2865-2873. doi: 10.1002/sim.3107.

Harris, F. J. (1978). On the use of windows for harmonic analysis with the discrete Fourier transform. *Proceedings of the IEEE*, *66*(1), 51-83. doi:10.1109/PROC.1978.10837.

Hassan, M., Dufor, O., Merlet, I., Berrou, C., & Wendling, F. (2014). EEG source connectivity analysis: from dense array recordings to brain networks. *PloS one*, *9*(8), e105041. doi:10.1371/journal.pone.0105041.

Huang, H. J., Kram, R., & Ahmed, A. A. (2012). Reduction of metabolic cost during motor learning of arm reaching dynamics. *Journal of Neuroscience*, *32*(6), 2182-2190. doi: 10.1523/JNEUROSCI.4003-11.2012

Hunter, T., Sacco, P., Nitsche, M. A., & Turner, D. L. (2009). Modulation of internal model formation during force field-induced motor learning by anodal transcranial direct current stimulation of primary motor cortex. *The Journal of physiology*, *587*(12), 2949-2961. doi: 10.1113/jphysiol.2009.169284.

Hyvärinen, A., Karhunen, J., & Oja, E. (2004). *Independent component analysis* (Vol. 46). John Wiley & Sons.

Jasper, H. (1958). Ten-twenty electrode system of the international federation. *Electroencephalogr. Clin. Neurophysiol., 10,* 371-375.

Kitago, T. O. M. O. K. O., & Krakauer, J. W. (2013). Motor learning principles for neurorehabilitation. *Handb Clin Neurol*, *110*, 93-103. doi: 10.1016/B978-0-444-52901-5.00008-3.

Koechlin, E., Basso, G., Pietrini, P., Panzer, S., & Grafman, J. (1999). The role of the anterior prefrontal cortex in human cognition. *Nature*, *399*(6732), 148-151. doi:10.1038/20178.

Kounios, J., Fleck, J. I., Green, D. L., Payne, L., Stevenson, J. L., Bowden, E. M., & Jung-Beeman, M. (2008). The origins of insight in resting-state brain activity. *Neuropsychologia*, *46*(1), 281-291. doi:10.1016/j.neuropsychologia.2007.07.013.

Krakauer, J. W., Ghilardi, M. F., Mentis, M., Barnes, A., Veytsman, M., Eidelberg, D., & Ghez, C. (2004). Differential cortical and subcortical activations in learning rotations and gains for reaching: a PET study. *Journal of neurophysiology*, *91*(2), 924-933. doi:10.1152/jn.00675.2003.

Krebs, H. I., Brashers-Krug, T., Rauch, S. L., Savage, C. R., Hogan, N., Rubin, R. H., ... & Alpert, N. M. (1998). Robot-aided functional imaging: Application to a motor learning

study. *Human brain mapping*, *6*(1), 59-72. doi: 10.1002/(SICI)1097-0193(1998)6:1<59::AID-HBM5>3.0.CO;2-K.

Krishnan, A., Williams, L. J., McIntosh, A. R., & Abdi, H. (2011). Partial Least Squares (PLS) methods for neuroimaging: a tutorial and review. *Neuroimage*, *56*(2), 455-475. doi:10.1016/j.neuroimage.2010.07.034.

Krishnan, L., Kang, A., Sperling, G., & Srinivasan, R. (2013). Neural strategies for selective attention distinguish fast-action video game players. *Brain topography*, *26*(1), 83-97. doi: 10.1007/s10548-012-0232-3.

Landi, S. M., Baguear, F., & Della-Maggiore, V. (2011). One week of motor adaptation induces structural changes in primary motor cortex that predict long-term memory one year later. *Journal of Neuroscience*, *31*(33), 11808-11813.

Lee, T. W., Girolami, M., & Sejnowski, T. J. (1999). Independent component analysis using an extended infomax algorithm for mixed subgaussian and supergaussian sources. *Neural computation*, *11*(2), 417-441.

Linkenkaer-Hansen, K., Nikouline, V. V., Palva, J. M., & Ilmoniemi, R. J. (2001). Long-range temporal correlations and scaling behavior in human brain oscillations. *The Journal of neuroscience*, *21*(4), 1370-1377.

Ludwig, K. A., Miriani, R. M., Langhals, N. B., Joseph, M. D., Anderson, D. J., & Kipke, D. R. (2009). Using a common average reference to improve cortical neuron recordings from microelectrode arrays. *Journal of neurophysiology*, *101*(3), 1679-1689. doi:10.1152/jn.90989.2008.

Maitra, S., & Yan, J. (2008). Principle component analysis and partial least squares: Two dimension reduction techniques for regression. *Applying Multivariate Statistical Models*, *79*.

Mary, A., Wens, V., Op de Beeck, M., Leproult, R., De Tiège, X., Peigneux, P. (2017). Resting-state Functional Connectivity is an Age-dependent Predictor of Motor Learning Abilities. Cerebral Cortex 27, 4923–4932. doi: 10.1093/cercor/bhw286.

Martens, H., & Martens, M. (2000). Modified Jack-knife estimation of parameter uncertainty in bilinear modelling by partial least squares regression (PLSR). *Food quality and preference*, *11*(1), 5-16. doi: 10.1016/S0950-3293(99)00039-7.

Martens, H., Næs, T. (1989). Multivariate calibration. Chichester: Wiley.

Mathewson, K. E., Basak, C., Maclin, E. L., Low, K. A., Boot, W. R., Kramer, A. F., ... & Gratton, G. (2012). Different slopes for different folks: alpha and delta EEG power predict subsequent video game learning rate and improvements in cognitive control tasks. *Psychophysiology*, *49*(12), 1558-1570. doi: 10.1111/j.1469-8986.2012.01474.x

Mehmood, T., Liland, K. H., Snipen, L., & Sæbø, S. (2012). A review of variable selection methods in partial least squares regression. *Chemometrics and Intelligent Laboratory Systems*, *118*, 62-69. doi: 10.1016/j.chemolab.2012.07.010.

Mehrkanoon, S., Boonstra, T. W., Breakspear, M., Hinder, M., & Summers, J. J. (2016). Upregulation of cortico-cerebellar functional connectivity after motor learning. *NeuroImage*, *128*, 252-263. doi: 10.1016/j.neuroimage.2015.12.052.

Molteni, E., Cimolin, V., Preatoni, E., Rodano, R., Galli, M., & Bianchi, A. M. (2012). Towards a biomarker of motor adaptation: Integration of kinematic and neural factors. *IEEE Transactions on Neural Systems and Rehabilitation Engineering*, *20*(3), 258-267.

Ng, K. S. (2013). A simple explanation of partial least squares.

Oostenveld, R., Fries, P., Maris, E., & Schoffelen, J. M. (2011). FieldTrip: open source software for advanced analysis of MEG, EEG, and invasive electrophysiological data. *Computational intelligence and neuroscience*, *2011*, 1. doi:10.1155/2011/156869.

Osu R., Burdet E., Franklin D. W., Milner T. E., Kawato M. (2003). Different mechanisms involved in adaptation to stable and unstable dynamics. J. Neurophysiol. 90, 3255–3269. 10.1152/jn.00073.2003. doi: 10.1152/jn.00073.2003.

Ozdenizci, O., Yalcin, M., Erdogan, A., Patoglu, V., Grosse-Wentrup, M., & Cetin, M. (2017). Electroencephalographic identifiers of motor adaptation learning. *Journal of Neural Engineering*. doi:10.1088/1741-2552/aa6abd.

Patton, J. L., & Mussa-Ivaldi, F. A. (2004). Robot-assisted adaptive training: custom force fields for teaching movement patterns. *IEEE Transactions on Biomedical Engineering*, *51*(4), 636-646. doi: 10.1109/TBME.2003.821035.

Pierna, J. A. F., Abbas, O., Baeten, V., & Dardenne, P. (2009). A Backward Variable Selection method for PLS regression (BVSPLS). *Analytica chimica acta*, *642*(1), 89-93. doi: 10.1016/j.aca.2008.12.002.

Pizzamiglio, S., De Lillo, M., Naeem, U., Abdalla, H., & Turner, D. L. (2017). High-Frequency Intermuscular Coherence between Arm Muscles during Robot-Mediated Motor Adaptation. *Frontiers in Physiology*, *7*. doi:10.3389/fphys.2016.00668.

R core team (2013). *R: A Language and Environment for Statistical Computing R Foundation for Statistical Computing*.

Rodgers, J. L., & Nicewander, W. A. (1988). Thirteen ways to look at the correlation coefficient. *The American Statistician*, *42*(1), 59-66.

Ramnani, N., & Owen, A. M. (2004). Anterior prefrontal cortex: insights into function from anatomy and neuroimaging. *Nature Reviews Neuroscience*, *5*(3), 184-194. doi:10.1038/nrn1343.

Riener, R., Lunenburger, L., Jezernik, S., Anderschitz, M., Colombo, G., & Dietz, V. (2005). Patient-cooperative strategies for robot-aided treadmill training: first experimental results. *IEEE transactions on neural systems and rehabilitation engineering*, *13*(3), 380-394. doi: 10.1109/TNSRE.2005.848628.

Reinkensmeyer, D. J., Burdet, E., Casadio, M., Krakauer, J. W., Kwakkel, G., Lang, C. E., ... & Schweighofer, N. (2016). Computational neurorehabilitation: modeling plasticity and learning to predict recovery. *Journal of neuroengineering and rehabilitation*, *13*(1), 1. doi: 10.1186/s12984-016-0148-3.

Salehi, M., Karbasi, A., Shen, X., Scheinost, D., & Constable, R. T. (2017). An exemplar-based approach to individualized parcellation reveals the need for sex specific functional networks. *NeuroImage*. doi: 10.1016/j.neuroimage.2017.08.068.

Shadmehr, R., & Holcomb, H. H. (1997). Neural correlates of motor memory consolidation. *Science*, *277*(5327), 821-825. doi:10.1126/science.277.5327.821.

Scheidt, R. A., & Stoeckmann, T. (2007). Reach adaptation and final position control amid environmental uncertainty after stroke. *Journal of neurophysiology*, *97*(4), 2824-2836.

Stinear, C. (2010). Prediction of recovery of motor function after stroke. *The Lancet Neurology*, *9*(12), 1228-1232. doi:10.1016/S1474-4422(10)70247-7.

Storey, B. D. (2002). Computing Fourier series and power spectrum with Matlab. *TEX paper*.

Tailby, C., Masterton, R. A., Huang, J. Y., Jackson, G. D., & Abbott, D. F. (2015). Resting state functional connectivity changes induced by prior brain state are not network specific. *NeuroImage*, *106*, 428-440.

Tambini, A., Ketz, N., & Davachi, L. (2010). Enhanced brain correlations during rest are related to memory for recent experiences. *Neuron*, *65*(2), 280-290. doi:10.1016/j.neuron.2010.01.001.

Tian, L., Wang, J., Yan, C., & He, Y. (2011). Hemisphere-and gender-related differences in small-world brain networks: a resting-state functional MRI study. *Neuroimage*, *54*(1), 191-202. doi: 10.1016/j.neuroimage.2010.07.066.

Tomassini, V., Jbabdi, S., Kincses, Z. T., Bosnell, R., Douaud, G., Pozzilli, C., ... & Johansen-Berg, H. (2011). Structural and functional bases for individual differences in motor learning. *Human brain mapping*, *32*(3), 494-508. doi: 10.1002/hbm.21037.

Trewartha, K. M., Garcia, A., Wolpert, D. M., & Flanagan, J. R. (2014). Fast but fleeting: adaptive motor learning processes associated with aging and cognitive decline. *Journal of neuroscience*, *34*(40), 13411-13421. doi:10.1523/JNEUROSCI.1489-14.2014.

Trygg, J., & Wold, S. (2002). Orthogonal projections to latent structures (O-PLS). *Journal of chemometrics*, *16*(3), 119-128. doi:10.1002/cem.695.

Tubau, E., Escera, C., Carral, V., & Corral, M. J. (2007). Individual differences in sequence learning and auditory pattern sensitivity as revealed with evoked potentials. *European Journal of Neuroscience*, *26*(1), 261-264.

Tulving, E. (1985). How many memory systems are there? *American psychologist*, *40*(4), 385. doi:10.1037/0003-066X.40.4.385.

Turner, D. L., Murguialday, A. R., Birbaumer, N., Hoffmann, U., & Luft, A. (2013). Neurophysiology of robot-mediated training and therapy: a perspective for future use in clinical populations. Frontiers in neurology, 4, 184. doi:10.3389/fneur.2013.00184.

Vahdat, S., Darainy, M., Milner, T. E., & Ostry, D. J. (2011). Functionally specific changes in resting-state sensorimotor networks after motor learning. *Journal of Neuroscience*, *31*(47), 16907-16915. doi: 10.1523/JNEUROSCI.2737-11.2011.

Wakeling, I. N., & Morris, J. J. (1993). A test of significance for partial least squares regression. *Journal of Chemometrics*, *7*(4), 291-304. doi:10.1002/cem.1180070407.

Wehrens, R. (2011). *Chemometrics with R: multivariate data analysis in the natural sciences and life sciences*. Springer Science & Business Media.

Wold, H. (1982). Soft modelling: the basic design and some extensions. *Systems under indirect observation, Part II*, 36-37.

Wold, S., Antti, H., Lindgren, F., & Öhman, J. (1998). Orthogonal signal correction of near-infrared spectra. *Chemometrics and Intelligent laboratory systems*, *44*(1), 175-185. doi:10.1016/S0169-7439(98)00109-9.

Wold, S., Sjöström, M., & Eriksson, L. (2001). PLS-regression: a basic tool of chemometrics. *Chemometrics and intelligent laboratory systems*, *58*(2), 109-130. doi:10.1016/S0169-7439(01)00155-1.

World Medical Association. (2002). World Medical Association Declaration of Helsinki. Ethical principles for medical research involving human subjects. Nursing Ethics, 9(1), 105.

Wu, J., Srinivasan, R., Kaur, A., & Cramer, S. C. (2014). Resting-state cortical connectivity predicts motor skill acquisition. *Neuroimage*, *91*, 84-90. doi:10.1016/j.neuroimage.2014.01.026.

Wu, J., Quinlan, E. B., Dodakian, L., McKenzie, A., Kathuria, N., Zhou, R. J., ... & Cramer, S. C. (2015). Connectivity measures are robust biomarkers of cortical function and plasticity after stroke. *Brain*, *138*(8), 2359-2369. doi: 10.1093/brain/awv156.

Yeniay, O., & Goktas, A. (2002). A comparison of partial least squares regression with other prediction methods. *Hacettepe Journal of Mathematics and Statistics*, *31*(99), 99-101.

Youssofzadeh, V., Zanotto, D., Wong-Lin, K., Agrawal, S., & Prasad, G. (2016). Directed Functional Connectivity in Fronto-Centroparietal Circuit Correlates with Motor Adaptation in Gait Training. doi:10.1109/TNSRE.2016.2551642.